Marine Micropaleontology 145 (2018) 21–27

Contents lists available at ScienceDirect

Marine Micropaleontology

journal homepage: www.elsevier.com/locate/marmicro

March SST reconstruction in the South China Sea based on *Pinus massoniana* tree-ring widths from Changting, Fujian, in Southeast China since 1893 CE

Shuai Yuan[a], Yonghong Zheng[a,*], Shengbiao Wu[b,c], Peng Xu[d], Fangfang Zhang[a], Fanxi Kong[a], Yongdong Qi[a], Dan Wang[a]

[a] School of Resources and Environmental Science, Wuhan University, Wuhan 430079, China
[b] State key laboratory of Remote Sensing Science, Institute of Remote Sensing and Digital Earth, Chinese Academy of Sciences, Beijing 100101, China
[c] College of Resources and Environment, University of Chinese Academy of Sciences, Beijing 100049, China
[d] School of Geography and Planning, Sun Yat-Sen University, Guangzhou 510275, China

ARTICLE INFO

Keywords:
Changting
South China Sea
Dendroclimatology
Pinus massoniana
SST reconstruction

ABSTRACT

To study regional climate change and sea surface temperature (SST) variations in the South China Sea, three tree-ring width index chronologies (whole ring width, earlywood width and latewood width) of the *Pinus massoniana* from Changting, Fujian, in Southeast China were built. A correlation analysis was conducted between the chronologies and climate variables, and the results demonstrated that the March SST correlation coefficients for earlywood and whole ring width chronologies for the period 1982–2011 were estimated to be 0.558 and 0.677, respectively, which were highly significant at the 0.01 confidence level. SSTs were reconstructed from 1893 to 2011 CE for the South China Sea. The reconstruction explained 45.9% of the variance during the calibration period (1982–2011). On a decadal timescale, for the reconstructed SSTs during the reliable period (1904–2011), above-mean temperature periods occurred in 1904–1913, 1929–1948, 1961–1973 and 1991–2006 CE, whereas below-mean temperature periods occurred in 1914–1925, 1949–1960, 1979–1990 and 2007–2011 CE. This reconstruction could aid in the evaluation of regional climate variability in the South China Sea.

1. Introduction

The South China Sea is located at the southern tip of China, which is in a unique geographical location. Sea Surface Temperatures (SSTs) in the South China Sea directly affect the outbreak time and burst intensity of the summer monsoon, which has a significant impact on China and its surrounding areas. In addition, several studies have revealed that SSTs in the South China Sea are closely related to climate change (Wu and Chen, 2015; Yan et al., 2012). However, due to the lack of SST observations, studies examining SST variability over the past one century and their influence on climate change in China are seriously lacking.

Paleoclimatic records can be applied to extend our understanding of the past climate. As one of the most important high-resolution proxies, tree-ring data plays an important role in reconstructing climate over the past hundreds (D'Arrigo et al., 2003; Gray et al., 2004; Wilson et al., 2005) and even thousands of years (Cook et al., 2002; Esper et al., 2002; Jones et al., 2001; Zhang et al., 2003). Recently, an increasing number of tree-ring studies have been performed to assess the relationship between tree-rings and the marine climate index, including SSTs in the Central Pacific (Liu et al., 2017) and Atlantic multidecadal variability in the North Atlantic (Wang et al., 2017). However, up until now, there have been very few studies regarding the reconstruction of SSTs based on the tree-ring width index, which is largely due to the scarcity of old trees and the complex relationships between the radial growth of trees and SSTs in the southeast regions of China.

In this study, we developed three tree-ring width chronologies using tree-ring cores from *Pinus massoniana* in Changting. The purpose was to supplement historical climatic reconstructions for the subtropical China region. The growth–climate relationship was then analyzed, and finally, SST variations from 1893 to 2011 were reconstructed. This study is the first tree-ring-based dendroclimatic SST reconstruction for the South China Sea, which represents centennial-long climatic information. We hope that this climatic information may help further our understanding of the behavior of SSTs and the characteristics of climate variability in the region over the past one century. In addition, considering many previous marine-based SST proxies such as corals (Zhang et al., 2009) and geoduck (Black et al., 2009), we hope that this method of using

* Corresponding author.
E-mail address: zhengyh@whu.edu.cn (Y. Zheng).

https://doi.org/10.1016/j.marmicro.2018.10.003
Received 12 November 2017; Received in revised form 17 October 2018; Accepted 28 October 2018
Available online 30 October 2018
0377-8398/

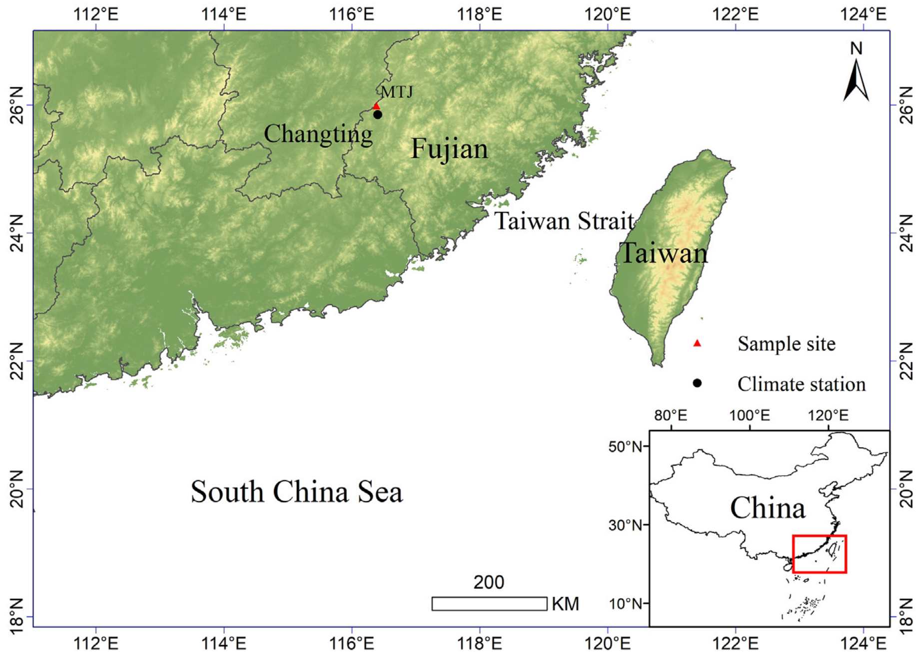

Fig. 1. Location of the research area.

only tree-rings to reconstruct SST can provide some useful references for research on marine biology in the future.

2. Data and methods

2.1. Research area

The research area is located south of the Wuyi Mountains in Fujian Province (Fig. 1). The growth of trees may be affected by the climatic conditions of the South China Sea, which is close to the study area. The region is influenced by the East Asian monsoon and has a humid subtropical monsoon climate characterized by warm winters, hot summers, little frost and snow, and sufficient rain and sunshine. The main wind is southerly in summer and northerly in winter. The meteorological station in Changting (25°51′N, 116°22′E, 311 m a.s.l.) recorded a 1981–2010 mean annual precipitation of 1685.6 mm and a mean annual temperature of 18.3 °C (Fig. 2). July is the warmest month in Changting with a mean temperature of 27.2 °C, and January is the coldest month with a mean temperature of 7.9 °C. The length of the frost-free period in Changting is 260 days. 70.5% of the annual precipitation falls during the growing season, which is approximately from April to September. There is a dry season from October to March.

Pinus massoniana is the most widely distributed and abundant species of pine tree in China. Natural *Pinus massiniana* forests are primarily distributed along the Qinling Mountains. *Pinus massiniana* is a dominant tree species in Fujian Province that generally grows 400 m a.s.l. Studies conducted in the Changting area have shown that *Pinus massiniana* is valuable for dendroclimatic research (Chen et al., 2012). Thus, this species provides an opportunity to conduct dendrochronological research in the subtropical region of Southeast China.

2.2. Tree-ring sampling and chronology development

We sampled trees at a site in Matouji (MTJ) within the Changting Region, on September 2012. The sampled trees were all from the *Pinus massoniana* forest. Except for individual trees, two core samples from opposite sides of each tree were extracted with 5-mm diameter increment borers at chest height. The sampling site was at 820 m a.s.l. and on northeast slopes, there was an inclination of 30–40° (Table 1).In total, 40 increment cores from 22 trees were sampled. The standard dendrochronology techniques (Cook and Kairiukstis, 2013) were used to process the sampled tree-ring cores.

In the Wuhan University laboratory, after air drying and mounting on wooden holders, increment cores were sanded with progressively finer grit sand-paper. After being visually cross-dated (Yamaguchi, 1991), the cores were measured to the nearest 0.001 mm by a LINTAB 6 tree-ring measurement station and the TSAP-Win program (Rinn, 2003). We measured the whole tree-ring width, the earlywood width and the latewood width of each core. Measurement errors and cross-dating were further checked with the computer program COFECHA

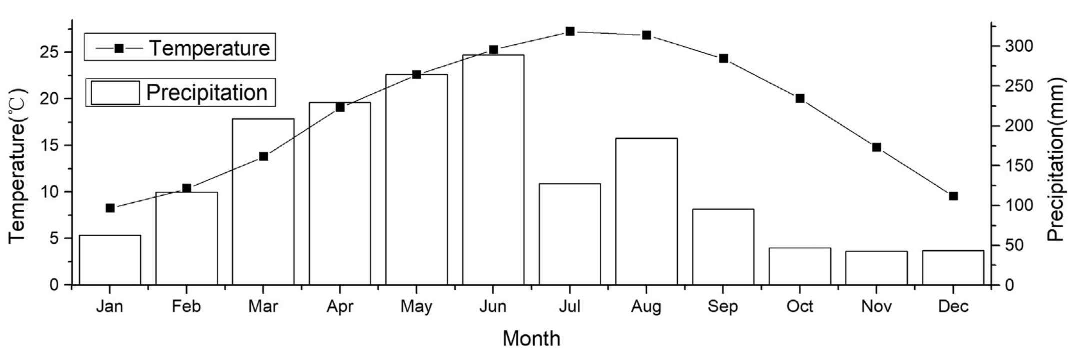

Fig. 2. Climate diagram for the Changting meteorological station from 1981 to 2010.

Table 1
Information about the sampling site in Changting.

Site	Lat. (N)	Long. (E)	Core/tree number	Elevation (m)	Aspect	Slope
MTJ	25°59′	116°24′	40/22	820	Northwest	30–40°

(Holmes, 1983). In the end, 39 increment cores from 22 trees were included in the final analysis. The chronology was developed using the program ARSTAN (Cook, 1985). All but one measured series were detrended using smoothing splines with a frequency–response cutoff set at two-thirds the length in order to remove nonclimatic, age-related growth trends (Cook and Kairiukstis, 2013). The remaining one latewood ring-width series, which contained anomalous growth trends, were detrended by fitting them to negative exponential curves. The ARSTAN program produced three versions of the standardized chronologies: standard, residual and arstan. We used the standard chronology, which contained common variations among individual tree core series and retained much lower frequency signals and is the most commonly used in tree-ring studies.

2.3. Climate data and statistical analysis

To analyze the relationship between the three standardized ring width chronologies and climate data, we tested several measured and modeled climate variables. Climate data were obtained from the Changting meteorological station (25°51′N, 116°22′E, 311 m a.s.l.) close to the sampling sites, which have recorded standard climatic parameters since 1956. Aside from standard climate parameters such as temperature and precipitation, we also tested the relationship with SSTs in the South China Sea, which is close to the sampling site. The SST data used in this paper was obtained from the official website (https://climexp.knmi.nl/home) of the Royal Dutch Meteorological Research Association. We used SST data from the gridded (1° resolution) NCEP OI v2 SST data set (1982-2011). Climate series from 16 grid points (112°–116°E, 16°–20°N) in the South China Sea were averaged to develop a regional time series.

The relationship between tree-ring width indexes and climate variables was investigated using Pearson's correlation in SPSS for the period 1956–2011. We chose an extended period of time (from October of the previous year to December of the current year) to analyze the growth climate relationship because climate variables may have a continued effect on growth in the current year and the following year.

To demonstrate our reconstruction's geographical representation, we conducted spatial correlations between our reconstructed SSTs and the gridded SST dataset from NCEP OI v2 for the period 1982–2011. The analyses were conducted using the KNMI climate explorer (http://www.knmi.nl).

3. Results

3.1. Three tree-ring width chronologies

Table 2 lists the statistics of the standard whole, earlywood and latewood ring-width chronologies. As we can see, the mean sensitivity (MS:0.126) and standard deviation (SD: 0.174) of the whole ring-width chronology were small, indicating rather moderate interannual variations in the ring-width series, which is characteristic of trees growing in humid and warm environments. The chronology exhibited typical autoregressive properties, with first-order autocorrelation coefficients averaging 0.620. The statistical results for EPS, SNR, and VFE were 0.856, 5.962, and 39.2%, respectively. These results indicate that the trees exhibited a common signal, which may be associated with the subtropical climate of China. Fig. 3c shows the whole ring–width index and sample depth. Although the first year in the chronology is 1893, the data were not reliable as a result of small subsample signal strength (SSS) values until 1904, at which point there were 10 cores with SSS values > 0.85, which means the chronology is reliable. The earlywood and latewood ring-width indexes are also below (Fig. 3a-b).

Table 2
Statistics of whole, earlywood, and latewood ring-width chronologies.

Statistical item	Whole	Earlywood	Latewood
Chronology period	1893–2011	1893–2011	1893–2011
Mean sensitivity (MS)	0.126	0.175	0.172
Standard deviation (SD)	0.174	0.204	0.218
First order autocorrelation	0.620	0.514	0.434
Signal-to-noise ratio (SNR)	5.962	5.255	7.749
Variance in first eigenvector (VFE)	39.2%	40.5%	33.5%
Expressed population signal (EPS)	0.856	0.840	0.886
First year where SSS > 0.85 (core number)	1904 (14)	1904 (13)	1904 (13)

3.2. Tree growth–climate relationships

Fig. 4a-b shows the correlation between earlywood, latewood, and whole ring-width chronologies and the mean temperature and precipitation. We can see for the whole ring-width chronology that there was no significant correlation between the obtained chronology and monthly precipitation, except for October and November of the previous year. All monthly temperatures were not significantly correlated with the ring-width series, except for November of the previous year and February and October of current years. The chronologies of earlywood and latewood were the same as the whole ring-width chronology in relation to mean temperature and precipitation. Fig. 4c shows the correlation between the three chronologies and SST in the South China Sea. The correlations between chronologies and all selected monthly SSTs were positive, except for that correlations between latewood chronology and SSTs in October and December of the previous year. An evident feature is that many monthly SSTs are significantly correlated with the ring-width series at the 0.05 confidence level. SSTs in October, November, and December of the previous year and March of the current year were significantly correlated with the earlywood ring-width series at the 0.01 confidence level. Correlation coefficients between March SSTs and the whole tree-ring and earlywood were 0.677 and 0.558, respectively (Fig. 4c). Obviously, March SSTs had the strongest correlation with the whole ring-width series (Fig. 4). Based on the aforementioned results, it is concluded that the radial growth of *Pinus massoniana* in the study area is sensitive to SST variation.

Based on the response of tree growth to climatic variables (Fig. 4), the SST was found to highlight the effects on tree growth. The correlation coefficient between the March SST and the whole tree-ring index was 0.677, which is highly significant at the 0.001 confidence level (Fig. 5a). This implies that averaged SSTs in March play a significant role in tree growth in Changting, especially regarding the growth of the whole tree-ring width. To further investigate the correlation of the standard ring-width series with the March SST, we conducted a first order differential treatment of the whole tree-ring width index and SST (Fig. 5b). After first order differential treatment, tree-ring width was positively correlated with SSTs in March of the current year. The correlation coefficient during 1983–2011 was 0.730, which is highly significant at the 0.001 confidence level. We also made a 21-year running correlation analysis between tree-ring width index and SSTs, and the correlations were all significant at the 0.05 confidence level during this period, which shown that the relationship between them was stable and reliable.

After comparison, we found that the correlation between the whole tree-ring width chronology and climatic factors was the strongest among the three chronologies (Fig. 4). A strong correlation (r = 0.677) between the whole ring-width chronology and SST allowed us to

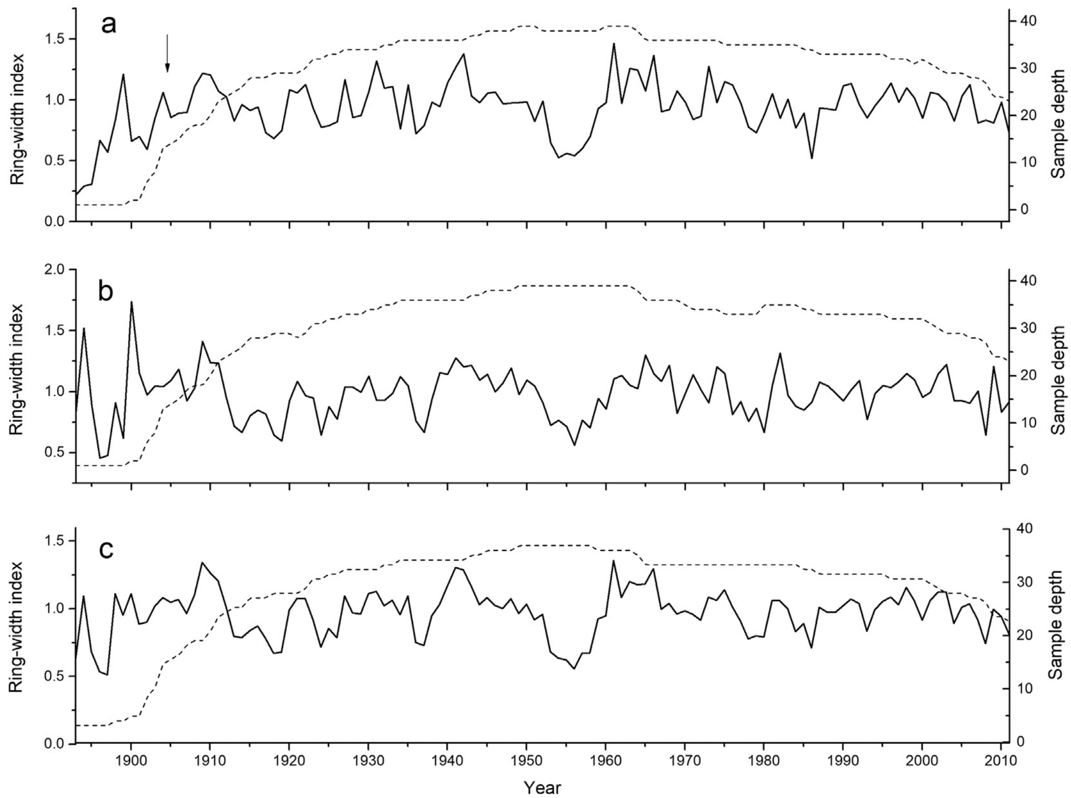

Fig. 3. Ring-width index (solid lines) and sample depth (dashed lines) for a) Earlywood, b) latewood and c) whole ring-width. Arrows denote the year with an SSS > 0.85.

reconstruct SSTs in March over the last one century. It was anticipated that our tree-ring based reconstruction in the region may reveal SST behaviors in the South China Sea.

3.3. Reconstruction of the March mean SST

Based on the results of the correlation analysis, the March mean SST was selected as the climate variable for reconstruction. Using a linear regression, the tree-ring index of the current year was chosen as the independent variable. The final transfer function was derived as

$$Y = 21.397 + 3.975 \times (R^2 = 0.459, p < .01)$$

where Y is the estimate of the March mean SST (in degrees Celsius), and X is the corresponding tree-ring index value. The reconstruction explained 45.9% of the temperature variation and 43.9% after the adjustment for the loss of degrees of freedom over the 1982–2011 interval. The statistical parameters of the transfer function, including reduction of error (RE = 0.384), standard error of estimate (SE = 0.490), F-value (23.871), demonstrated relatively good predictive capability of the transfer function.

Fig. 6 shows the observed and reconstructed March mean SST series. There was a very strong association between the two series, and the correlation between the two series was 0.677 during 1982–2011, which was highly significant at the 0.01 level. They showed very close similarity to each other.

4. Discussion

4.1. Tree growth-climate relationship at the study site

A positive relationship indicates that precipitation availability from October to November, which is before the growing season and occurs at the root zone of the tree, served as a booster and promoted tree growth. Except for October and November of the previous year, there was no significant correlation between the obtained chronology and precipitation for any month of the year, which agrees with previous studies (Chen et al., 2012). This result is because precipitation is not a limiting factor for tree growth in humid regions, especially at high mountainous altitudes in humid regions (Massaccesi et al., 2008; Savva et al., 2006).

As we know, the increase in atmospheric temperature advances the recovery time of the formation layer, thus prolonging the growth period of trees (Deslauriers et al., 2008). From January to March, rising temperatures can make the Changting spring begin ahead of time, which can accelerate the earlywood growth of *Pinus massoniana*. In October, *Pinus massoniana* is in the late stages of growth. The elevated temperature can prolong the growth period of *Pinus massoniana*, which can lead to an increase in the whole ring-width. In other months, the temperature range remained suitable for growth, so the change in temperature had no obvious restriction on the growth of *Pinus massoniana*. In summer, especially in July, temperatures were higher, and precipitation was insufficient. The rising temperature may cause an increase in soil evaporation, which can reduce water supply. At the same time, high temperatures can accelerate tree metabolism and increase transpiration, leading to moisture stress on tree growth. This also occurs in the late growth stages of earlywood and early stages of latewood, so the whole, earlywood and latewood widths were negatively correlated with July air temperatures. In addition, same with previous study (Chen et al., 2012), we found that the temperature from November of the previous year to February of the current year significantly correlated with tree-ring width index of our standard and residual chronology at the 0.05 confidence level. But we still found that the SSTs and the tree-ring width index of standard chronology had a better correlation, which shows that the reconstructed SSTs are suitable.

The results of the correlation analysis (Fig. 4) suggest that the radial growth of *Pinus massoniana* in Changting in subtropical central China

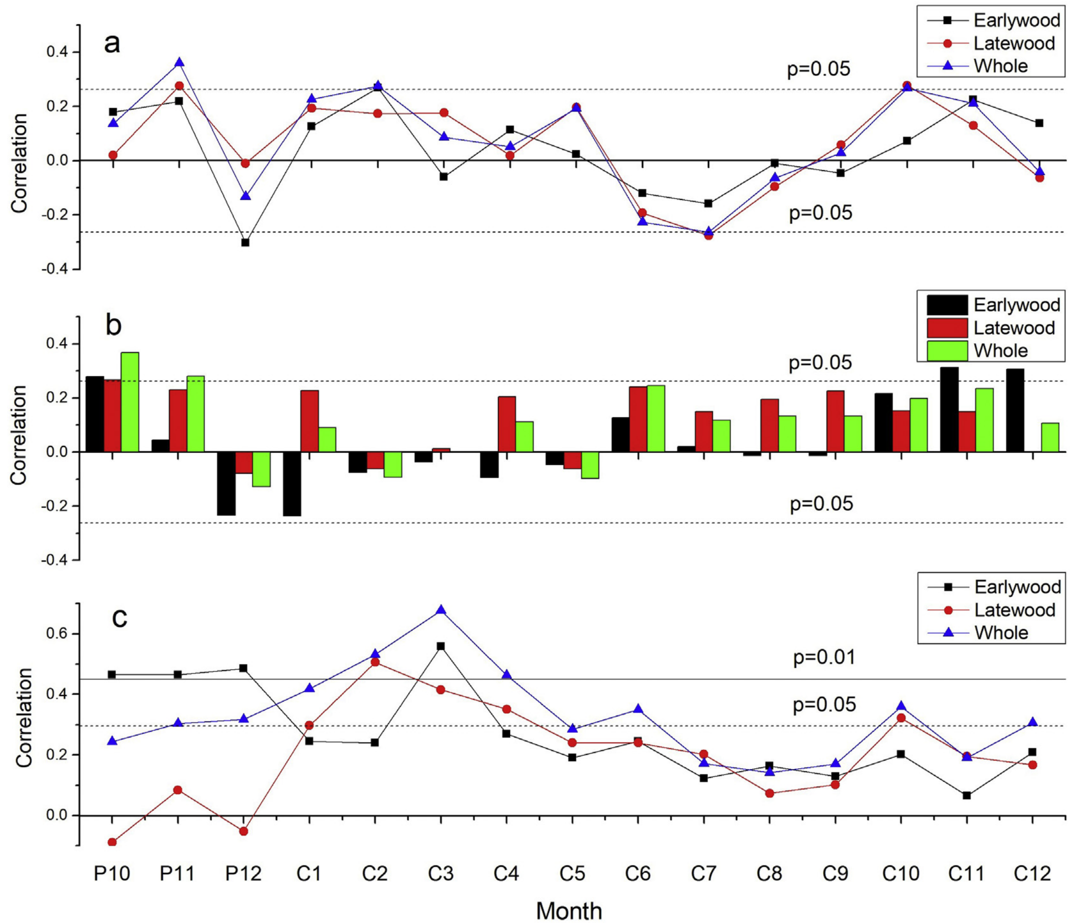

Fig. 4. Correlation coefficients for earlywood, latewood and the whole standard ring-width series with a) mean temperature, b) precipitation, and c) SST in the South China Sea. Solid lines and dashed lines indicate significance levels of $p < .05$ and $p < .01$, respectively. P represents the previous year, and C represents the current year.

was influenced not only by temperature and precipitation but also by other climatic parameters. The results indicate that March SSTs greatly affect tree growth. There were positive correlations between spring SSTs and tree growth. The seasonal disparity was mainly caused by local climatic conditions. Part of the water vapor in this area originates from the South China Sea, which can directly affect the growth of trees. In addition, the increase in SST is one of the main reasons for the rise in ground temperature and moisture content, which is undoubtedly

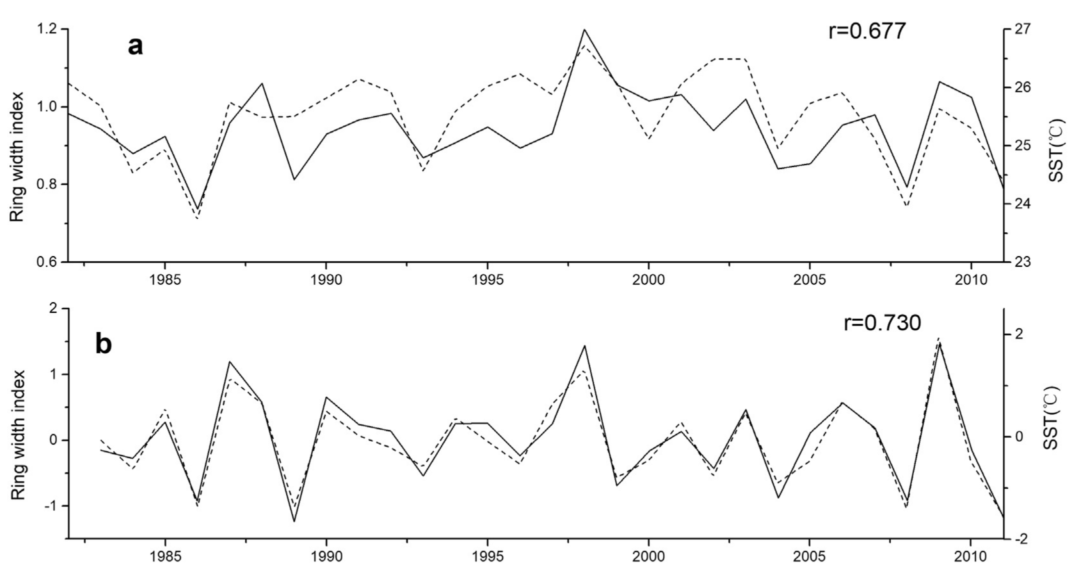

Fig. 5. a) Ring width index of the standard whole ring-width series (dashed line) and March SSTs (solid line) and b) the standard whole ring-width series (dashed line) and March SSTs (solid line) after the first order differential treatment.

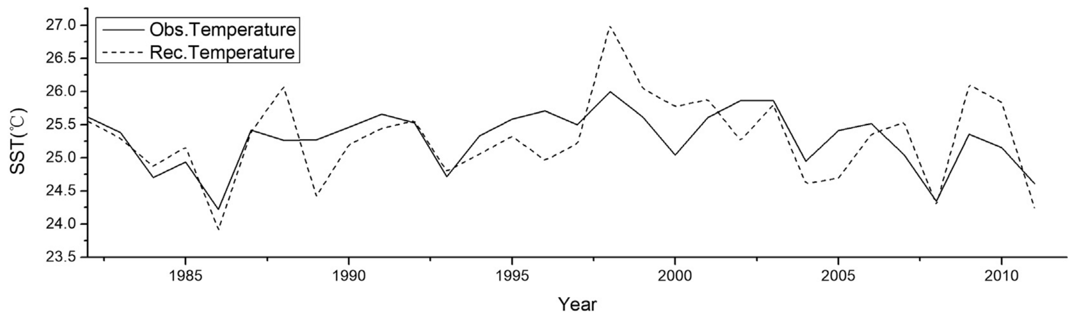

Fig. 6. Comparison between the observed and reconstructed March SSTs.

conducive to a tree's earlywood growth. Furthermore, that generation of earlywood affects latewood growth to a certain degree; thus, the whole ring-width index was highly correlated with SST. In summary, we can draw the conclusion that SSTs in March play a more important role than those in other months in whole ring-width radial growth, according to the growth-climate response relationship.

4.2. Reconstructed March SSTs and spatial extent

The reconstructed March SSTs provide estimates of 119 years of SST variability in the South China Sea (Fig. 7). The smoothed line represents an 11-year running mean of reconstructed SST to emphasize the variance on decadal and intra decadal scales over the last 119 years (Fig. 7). The mean reconstructed temperature was 25.24 °C. For the past 108 years, when the chronology is considered reliable, the warm periods included 1904–1913, 1929–1948, 1961–1973 and 1991–2006 CE, while the cool periods mainly included 1914–1925, 1949–1960, 1979–1990 and 2007–2011 CE. Obvious cold periods from reconstructed SSTs in the 20th century were observed during 1914–1925 and 1949–1960 CE. A western Pacific warm pool from an SST reconstruction detected in a previous study (March–July) was also reflected in the two observed cold periods (Zhang et al., 2009). Some differences in the reconstruction might be due to either the geographical setting or the types of proxies.

Spatial correlations between our reconstruction and the gridded SST dataset from NCEP OI v2 reveal our record's reliability and representativeness (Fig. 8). The reconstructed SSTs show a significant correlation ($r > 0.600$, $p < .01$) with the March SST from the NCEP OI v2 dataset in most regions of the South China Sea for the period 1983–2011. These results confirm that our reconstruction captures broad-scale regional climatic variations. In addition, our reconstruction showed significant correlations with the March SST NCEP OI v2 dataset in the northern regions of the Indian Ocean (Fig. 8). Further studies are needed to assess whether the radial growth of trees in our study area has a certain response to climate change in the Indian Ocean.

4.3. Response of earlywood growth of trees to climate change

In this study, earlywood, latewood and whole ring width chronologies were separately correlated with climate to explore the complex relationship between tree growth and climate. Although the whole width chronologies showed a stronger correlation, the impact of SSTs on the growth of earlywood cannot be ignored. The correlation coefficients between October and November SSTs of the previous year and the earlywood index was 0.531, which was highly significant at the 0.01 confidence level. As we know, increased winter temperatures may mean less damage to roots and leaves during the winter and, thus, less growth limitation. A previous study found positive correlations between winter air temperatures in eastern China and SSTs in the Pacific Ocean (Chen et al., 2009). Therefore, the relationship between earlywood and SST may reveal that winter SSTs play an important role in the growth of *Pinus massoniana* in Changting, Southeast China.

5. Conclusions

In this study, the high correlation between whole ring widths and SSTs indicates that the growth of trees at the chosen site was greatly affected by the SSTs in the South China Sea. Therefore, we reconstructed March SSTs in the South China Sea using tree-ring widths from *Pinus massoniana* in Changting Fujian Province of Southeast China, which revealed variations from interannual to decadal scales over the past 119 years. It is the first tree-ring-based dendroclimatic SST (March) reconstruction for the South China Sea, where long-term SST records have been lacking up until now. Evaluating the behavior of SSTs over the South China Sea for the last one century was found to be useful. Thus, it further clarifies the relationship between tree growth and climate and determines which type of climate has the greatest influence on tree growth. This reconstruction could aid in the evaluation of regional climate variability in the South China Sea and this terrestrial-based approach of extending the history of reconstructed SSTs for the South China Sea using tree-ring width could help decade to millennial scale research on marine sediment cores in the future. However, a reconstruction extending back to 1893 CE is insufficiently long for

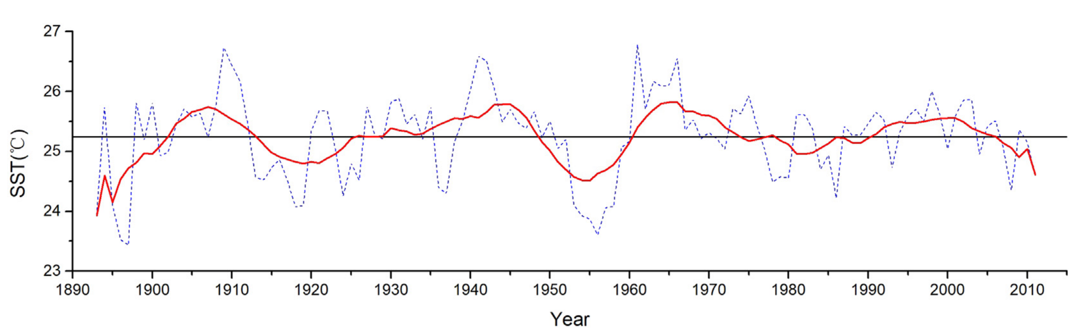

Fig. 7. March SST reconstruction from 1893 to 2011 for the South China Sea. The blue dashed curve represents the reconstruction, the red soild curve is an 11-year running mean of the reconstructed SST. (For interpretation of the references to colour in this figure legend, the reader is referred to the web version of this article.)

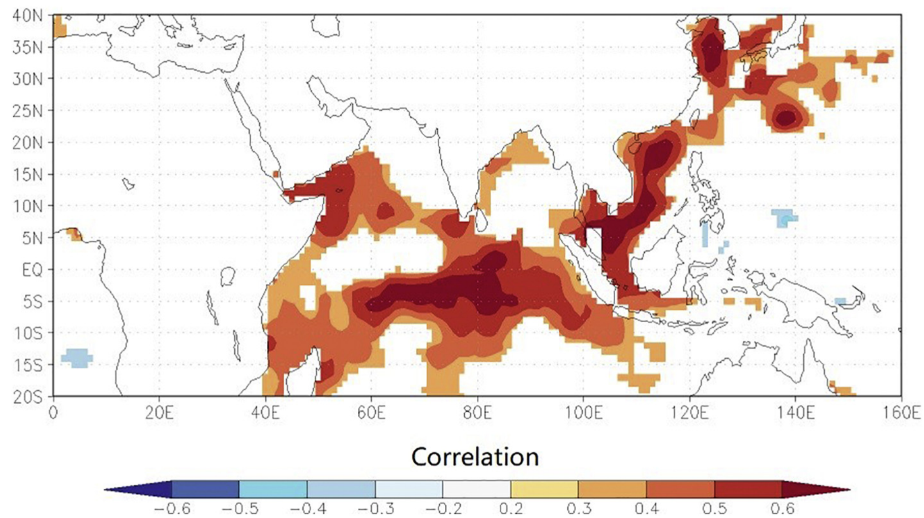

Fig. 8. Spatial correlation patterns of the SST reconstruction in the South China Sea, with the gridded NCEP OI v2 dataset for March SSTs, for the period 1983–2011.

studying long-term climate variability/change in depth and because of the relatively warm and humid climate in subtropical China, the rapid metabolism of trees resulted in a phenomenon where there were few trees older than 200 years in the study area. Thus, more effort should be made to develop tree-ring chronologies by collecting old trees in Southeast China to extend the reconstructed history of climate change.

Acknowledgments

This work was supported by the National Natural Science Foundation of China (Grant No. 41771227). The authors thank Wang Chen for his help.

References

Black, B.A., Copenheaver, C.A., Frank, D.C., Stuckey, M.J., Kormanyos, R.E., 2009. Multi-proxy reconstructions of northeastern Pacific Sea surface temperature data from trees and Pacific geoduck. Paleogeogr. Paleoclimatol. Paleoecol. 278, 40–47.
Chen, S.Y., Zhang, Y.X., Xia, Q., Bai, D.Y., Zhang, X.F., 2009. Analysis of relationship between winter air temperature in eastern china and sea surface temperature anomaly. Plateau Meteorol. 28, 1181–1188.
Chen, F., Yuan, Y.J., Wei, W.S., Yu, S.L., Zhang, T.W., 2012. Tree ring-based winter temperature reconstruction for Changting, Fujian, subtropical region of Southeast China, since 1850: linkages to the Pacific Ocean. Theor. Appl. Climatol. 109, 141–151.
Cook, E.R., 1985. A Time Series Analysis Approach to Tree Ring Standardization. The University of Arizona.
Cook, E.R., Kairiukstis, L.A., 2013. Methods of Dendrochronology: Applications in the Environmental Sciences. Springer Science & Business Media.
Cook, E.R., Palmer, J.G., D'Arrigo, R.D., 2002. Evidence for a 'medieval warm period' in a 1,100 year tree-ring reconstruction of past austral summer temperatures in New Zealand. Geophys. Res. Lett. 29, 4.
D'Arrigo, R.D., Cook, E.R., Mann, M.E., Jacoby, G.C., 2003. Tree-ring reconstructions of temperature and sea-level pressure variability associated with the warm-season Arctic Oscillation since AD 1650. Geophys. Res. Lett. 30, 4.
Deslauriers, A., Rossi, S., Anfodillo, T., Saracino, A., 2008. Cambial phenology, wood formation and temperature thresholds in two contrasting years at high altitude in southern Italy. Tree Physiol. 28, 863–871.
Esper, J., Cook, E.R., Schweingruber, F.H., 2002. Low-frequency signals in long tree-ring chronologies for reconstructing past temperature variability. Science 295, 2250–2253.
Gray, S.T., Graumlich, L.J., Betancourt, J.L., Pederson, G.T., 2004. A tree-ring based reconstruction of the Atlantic Multidecadal Oscillation since 1567 AD. Geophys. Res. Lett. 31, 4.
Holmes, R.L., 1983. Computer-assisted quality control in tree-ring dating and measurement. Tree-Ring Bull. 43, 69–78.
Jones, P.D., Osborn, T.J., Briffa, K.R., 2001. The evolution of climate over the last millennium. Science 292, 662–667.
Liu, Y., Cobb, K.M., Song, H.M., Li, Q., Li, C.Y., Nakatsuka, T., An, Z.S., Zhou, W.J., Cai, Q.F., Li, J.B., Leavitt, S.W., Sun, C.F., Mei, R.C., Shen, C.C., Chan, M.H., Sun, J.Y., Yan, L.B., Lei, Y., Ma, Y.Y., Li, X.X., Chen, D.L., Linderholm, H.W., 2017. Recent enhancement of Central Pacific El Nino variability relative to last eight centuries. Nat. Commun. 8, 8.
Massaccesi, G., Roig, F.A., Pastur, G.J.M., Barrera, M.D., 2008. Growth patterns of *Nothofagus pumilio* trees along altitudinal gradients in Tierra del Fuego, Argentina. Trees 22, 245–255.
Rinn, F., 2003. TSAP-Win: Time Series Analysis and Presentation for Dendrochronology and Related Applications. Frank Rinn, Heidelberg, Germany.
Savva, Y., Oleksyn, J., Reich, P.B., Tjoelker, M.G., Vaganov, E.A., Modrzynski, J., 2006. Interannual growth response of Norway spruce to climate along an altitudinal gradient in the Tatra Mountains, Poland. Trees 20, 735–746.
Wang, J.L., Yang, B., Ljungqvist, F.C., Luterbacher, J., Osborn, T.J., Briffa, K.R., Zorita, E., 2017. Internal and external forcing of multidecadal Atlantic climate variability over the past 1,200 years. Nat. Geosci. 10, 512.
Wilson, R.J.S., Luckman, B.H., Esper, J., 2005. A 500 year dendroclimatic reconstruction of spring-summer precipitation from the lower Bavarian Forest region, Germany. Int. J. Climatol. 25, 611–630.
Wu, R.G., Chen, Z., 2015. Intraseasonal SST variations in the South China Sea during boreal winter and impacts of the East Asian winter monsoon. J. Geophys. Res.-Atmos. 120, 5863–5878.
Yamaguchi, D.K., 1991. A simple method for cross-dating increment cores from living trees. Can. J. For. Res.-Rev. Can. Rech. For. 21, 414–416.
Yan, Y.F., Qi, Y.Q., Zhou, W., 2012. Variability of tropical cyclone occurrence date in the South China Sea and its relationship with SST warming. Dyn. Atmos. Oceans 55-56, 45–59.
Zhang, Q.B., Cheng, G.D., Yao, T.D., Kang, X.C., Huang, J.G., 2003. A 2,326-year tree-ring record of climate variability on the northeastern Qinghai-Tibetan Plateau. Geophys. Res. Lett. 30, 4.
Zhang, Z.Y., Gong, D.Y., He, X.Z., Guo, D., Feng, S.H., 2009. Reconstruction of the western Pacific warm pool SST since 1644 AD and its relation to precipitation over East China. Sci. China Ser. D Earth Sci. 52, 1436–1446.